

The effect of series elasticity on actuator power and work output: Implications for robotic and prosthetic joint design

Daniel Paluska^{a,*}, Hugh Herr^b

^a *Mechanical Engineering, The Media Lab, Massachusetts Institute of Technology, Cambridge, MA 02139, United States*

^b *The Media Lab, MIT-Harvard Division of Health Sciences and Technology, Massachusetts Institute of Technology, Cambridge, MA 02139, United States*

Received 15 October 2005; received in revised form 20 February 2006; accepted 21 February 2006

Available online 27 June 2006

Abstract

Evidence from biomechanics research suggests that tendon series elasticity allows muscle to act in an optimal range of its force–length and force–velocity curves to achieve work and power amplification. In this investigation we put forth a simple model to quantify the capacity of series elasticity to increase work and power output from an actuator. We show that an appropriate spring constant increases the energy that an actuator can deliver to a mass by a factor of 4. The series elasticity changes the actuator operating point along its force–velocity curve and therefore affects the actuator work output over a fixed stroke length. In addition, the model predicts that a series spring can store energy and deliver peak powers greater than the power limit of the source by a factor of 1.4. Preliminary experiments are performed to test model predictions. We find qualitative agreement between the model and experimental data, highlighting the importance of series elasticity for actuator work and power amplification across a fixed stroke length. We present several non-dimensional relations that can aid designers in the fabrication of robotic and prosthetic limbs optimized for work and power delivery.

© 2006 Elsevier B.V. All rights reserved.

Keywords: Series elasticity; Catapult; Actuation; Power amplification; Work amplification

1. Introduction

Biomechanists have noted that tendon series elasticity is important for energetic and efficiency purposes [1–8]. Roberts and Marsh [5] developed a simple model of a frog jumping that showed the benefits of series elasticity on muscle work output. They hypothesized that series elasticity changes the operating velocity and set-point of the muscle belly for certain tasks. In their model, total muscle work output while acting to accelerate an inertial load is increased with the appropriate series elasticity. Peak power delivered to the inertial load is also increased. Given the appropriate elasticity, their model states that the muscle-tendon unit was capable of greater power and work output than the muscle alone.

Robotics researchers have noted the importance of series elasticity for force control purposes [9–15] and also for energy

storage and release during running or hopping [16–18]. In the case of force control, the elasticity helps to reduce the output impedance of the actuator and acts as a mechanical low-pass filter for shocks. In the hoppers and runners, the elasticity provides efficient energy storage and release, enhancing the potential and kinetic energy exchange for such gaits.

In this paper we study how series elasticity affects actuator work and power output. We present a simple model that quantifies how series elasticity, actuator force–velocity limitations and load impedance affect actuator work and power output. Specifically, we are interested in how series elasticity influences a source like an electric motor, which has a force–velocity limitation but no force–length limitation.

We perform simulations of a mass being accelerated over a limited stroke length. This is analogous to the task of jumping from a crouched posture or throwing a ball from the chest. We simulate two cases. In Case 1, we begin with a force–velocity limited force source and simulate how much work is done on a mass over a limited stroke length. In Case 2, we insert series elasticity between the source and the load and, once again,

* Corresponding author.

E-mail addresses: leinad@media.mit.edu (D. Paluska), herr@media.mit.edu (H. Herr).

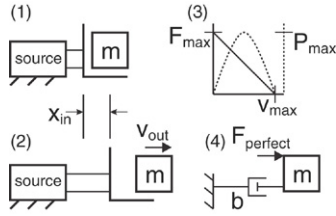


Fig. 1. Case 1: a bandwidth limited force source with a limited stroke x_{in} throws a mass m . Subfigures 1 and 2 show the beginning and end stages of the system launching an inertial load. Subfigure 3 shows the first-order force–velocity limitation and the power output of the source. P_{max} occurs at $V_{max}/2$ and is equal to $F_{max}V_{max}/4$. This can also be thought of as a first-order model of DC electric motor limitations. Subfigure 4 shows the linear bandwidth limitation modeled as a perfect force source in parallel with a damper of appropriate damping ratio, $b = F_{max}/V_{max}$.

simulate how much work the source does over a limited stroke length. A series elastic actuator is constructed, and pilot data are collected to compare with model predictions.

2. Simple models of actuator power and energy delivery

For Case 1, we consider a simple model to look at how an actuator delivers energy to launch a mass. Here a linear actuator is presented with a stroke length x_{in} and some first-order bandwidth limitations, specified by F_{max} and V_{max} . This can also be represented as a perfect source in parallel with a damper to ground, where $b = F_{max}/V_{max}$ (see Fig. 1). This limitation can be thought of as a first-order approximation of the limitations of a DC electric motor, biological muscle or fluid power source.

Consider the amount of energy that the actuator can impart to a mass, m , over the stroke of the actuator. Assuming that the mass starts at rest, the final energy is simply defined by the velocity at $x = x_{in}$. Here we examine the relationship between m , b , F_{max} , x_{in} , and the exit velocity, v .

Our source can command the force, but the load will determine the velocity. The optimal output (maximum power at all times) from the actuator is simply the maximum force given the velocity of the endpoint as determined by the interaction with the load. We can model this using a perfect (i.e. not velocity limited) force actuator in parallel with an appropriate damper. Given a step input in force of magnitude F_{max} , the actuator always acts along the line defined by the force–velocity limitation (Fig. 1, Part 3).

Consider the system in Fig. 1, part 4, when acted upon by a step function of input force, F_{max} . A single differential equation defines the system dynamics:

$$m\ddot{x} = F_{max} - b\dot{x}. \quad (1)$$

This equation can easily be solved for the time trajectories of the mass:

$$x(t) = V_{max}t + V_{max}\tau(-1 + e^{-t/\tau}) \quad (2)$$

$$\dot{x}(t) = V_{max}(1 - e^{-t/\tau}). \quad (3)$$

Eqs. (1) and (2) can be combined to develop a relationship between the actuator stroke and the exit velocity (energy of the

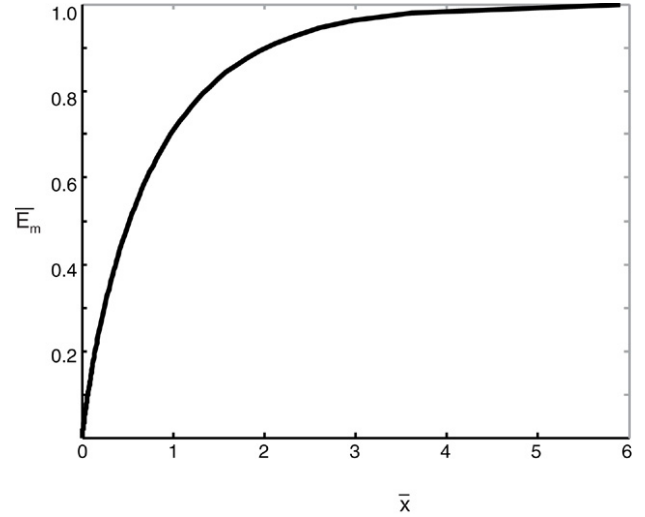


Fig. 2. Normalized energy delivery to a mass in Case 1. The x axis is the normalized actuator stroke, \bar{x}_{stroke} . The y axis is the normalized energy of the mass at the extent of the stroke, $\bar{E}_m = E/0.5mV_{max}^2$.

mass). By inverting the velocity equation to solve for t and then plugging this back into the position equation, we find

$$\begin{aligned} t &= -\tau \ln(1 - \dot{x}/V_{max}) \\ x &= -\tau V_{max} \ln\left(1 - \frac{\dot{x}}{V_{max}}\right) - \tau \dot{x} \\ \tau &= \frac{m}{b} = \frac{mV_{max}}{F_{max}} \end{aligned} \quad (4)$$

$$\bar{x}_{stroke} = -\ln(1 - \bar{x}_{exit}) - \bar{x}_{exit} \quad (5)$$

where $\bar{x}_{stroke} = x/\frac{mV_{max}^2}{F_{max}}$ and $\bar{x}_{exit} = \dot{x}/V_{max}$. \bar{x}_{stroke} is the normalized stroke length of the actuator. \bar{x}_{exit} is the normalized exit velocity of the mass. We can look more closely at this dimensionless relation in Eq. (5). If F_{max} increases, a shorter stroke is required to reach a given velocity. If m increases, a longer stroke is required. If V_{max} increases, a longer stroke is required. But this assumes that \bar{x}_{exit} stays constant, meaning that the exit velocity \dot{x} actually increases, since V_{max} increased.

Fig. 2 shows the energy delivered (actuator work done) for a given normalized stroke length, \bar{x}_{stroke} . The maximum possible energy delivered as $\bar{x}_{stroke} \rightarrow \infty$ is $E = 0.5mV_{max}^2$. In other words, the velocity limitation of the actuator and the mass define the ultimate limit of actuator work.

3. Adding series elasticity

For Case 2, we add a spring between the actuator and the mass, as shown in Fig. 3. The actuator has the same force–velocity limitation. For this case, we have simply added a passive elastic element, with stiffness k , between the actuator and the mass. We now have a second-order system that can be represented with the state variables v_{mass} and Δx . The following relations govern the system:

$$\Delta \dot{x} = x_{mass} - x_{source}$$

$$F_{max} - b\dot{x}_{source} = -k\Delta x$$

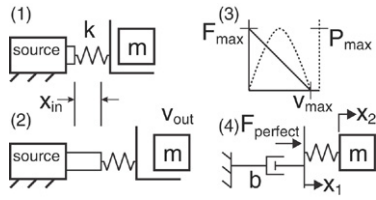


Fig. 3. Case 2. Series elasticity is inserted between the actuator and the mass. Subfigure 3 defines the actuator limitations and power output as in Case 1. Subfigure 4 once again models the limited source as an unlimited force source in parallel with an appropriate damper.

$$m\dot{v}_{\text{mass}} = -k\Delta x$$

$$v_{\text{mass}} = \dot{x}_{\text{mass}}$$

F_{max} is the perfect force source input and Δx is a measure of the elastic element strain.

Choosing Δx and v_{mass} as the state variables, we derive the following transfer functions:

$$\frac{\Delta x}{F_{\text{max}}} = \frac{s}{s^2 + \frac{k}{b}s + \frac{k}{m}} \quad (6)$$

$$\frac{v_{\text{mass}}}{F_{\text{max}}} = \frac{\frac{k}{mb}}{s^2 + \frac{k}{b}s + \frac{k}{m}} \quad (7)$$

To put k in dimensionless form, we normalize by b^2/m . This non-dimensional stiffness is related to the commonly used dimensionless damping ratio (ζ) parameter from system dynamics:

$$\bar{k} = \frac{k}{b^2/m} = \frac{km}{b^2} = \frac{1}{4\zeta^2}$$

3.1. Simulation methods

State Eqs. (6) and (7) for the system were integrated using *lsim* in MATLAB. This resulted in the state variables (and other dependent variables) as a function of time. These time data were then reordered into data based on source output position. Simulations were run for a variety of values of \bar{k} . The left graph in Fig. 4 was created by stepping through values of \bar{x}_{stroke} and selecting the maximum value of \bar{E} of all the trials at different \bar{k} values.

3.2. Simulation results

Fig. 4 shows the actuator work as a function of various series spring constants. For sufficiently large values of \bar{k} , the system is identical to Case 1. The right subfigure in Fig. 4 shows the envelope of all the maximum energies as a function of \bar{x}_{stroke} . At $\bar{x}_{\text{stroke}} \approx 0.5$, Case 1 and Case 2 actuator work curves deviate. In addition, $\bar{k} \gg 1$ will not increase actuator work output over any \bar{x}_{stroke} because we are approaching Case 1.

It is important to note that, for certain spring constants, there will be potential energy in the spring at the extent of the actuator travel. Here it is assumed that the actuator holds its position at the point of maximum travel while the spring extends and transfers all of its potential energy to the mass. Fig. 5 shows

the actuator force exerted on the spring–mass system as a function of the actuator displacement. The area under the force curve is a measure of the energy delivered to the spring–mass system. This area is the total actuator work done (see Fig. 4). In general, as \bar{x}_{stroke} increases, the optimal \bar{k} tends to decrease. This relationship is shown in Fig. 6.

3.3. Catapults

Is the spring in Case 2 acting like a catapult? We define a catapult as a system where a limited power source injects a certain amount of energy into a spring (winds it up) and then the spring releases that energy at a rate higher than the source can produce. Fig. 7 shows the motor power and the spring output power to the mass. There is a slight power amplification for certain values of k . This peaks at $k = 2$ and the amplification is roughly 1.4 or $\sqrt{2}$. For our model, we also assume that the actuator force and power will never be negative. The mass will simply be released before the end of travel.

Here we describe a simple model to extend this work to examine another catchless catapult. Consider the energy delivered with a wind-up and throw. This is analogous to an athlete bringing a ball backwards in order to wind-up before throwing the ball forward. The kinetic energy of the ball moving backwards is put into stretching the tendons. Then, as the athlete swings his arm forward, the stored energy in the tendons and additional muscle work propels the ball forward. If timed correctly, energy can be put into the tendons in both directions. Also, the second half of the motion will be on a different portion of the force–velocity curve. Fig. 8 shows an example of a wind-up and throw. The level of power amplification would depend on relative component values and the number of wind-ups. In the end, the peak actuator force will limit the number of wind-ups before the source will no longer be able to impart more energy into the spring mass system.

4. Work and power amplification experiments

Preliminary experiments were performed to evaluate the model. A diagram of the experimental setup is shown in Fig. 9. A photo of the apparatus can be seen in Fig. 10. The mechanical portion of our test setup consists of a series elastic actuator that uses a Maxon RE-40 brushed DC motor with a 13/3 gearhead, a 500 count shaft encoder, two equal timing pulleys, and a NSK 10 mm \times 4 mm ballscrew. The actuator is similar in physical layout to those described in Robinson et al. [19]. The actuator has a stroke length of 0.07 m (2.8 in.). The series springs are several different die springs. The actuator is mechanically grounded and pushes on a platform which is guided and supported by linear recirculating ball bearings. The platform weighs 10 kg (21 lbs).

Our electronics and control system is based around a PC/104 (Advanced Digital Logic) running the MATLAB XPC real-time operating system. There is an additional board (Sensoray) that provides an encoder counter, digital to analog (D/A) and analog to digital (A/D). The PC/104 system communicates the desired motor current to a motor amplifier (Copley Controls Accelus

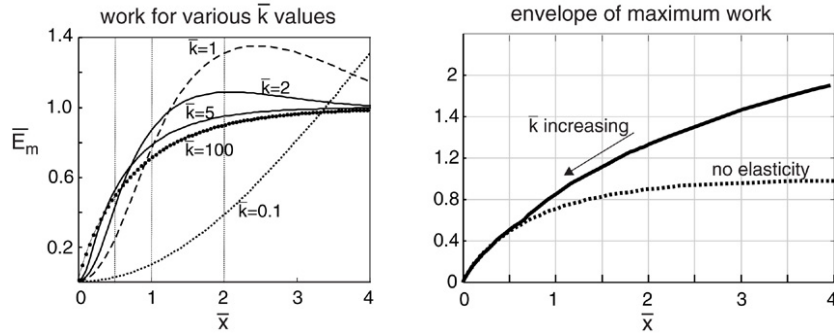


Fig. 4. Normalized energy delivery to a mass in the case with series elasticity. The x axis is the normalized actuator stroke, \bar{x}_{stroke} . The y axis is the normalized energy of the mass at the extent of the stroke, \bar{E}_m . The energy delivery is plotted for various values of dimensionless series elasticity, \bar{k} . As \bar{k} becomes large, the plot approaches Case 1. The figure on the right shows the maximum energy envelope, \bar{E} , given the stroke \bar{x}_{stroke} . As \bar{k} decreases and \bar{x}_{stroke} increases, $\bar{E} \rightarrow 4$.

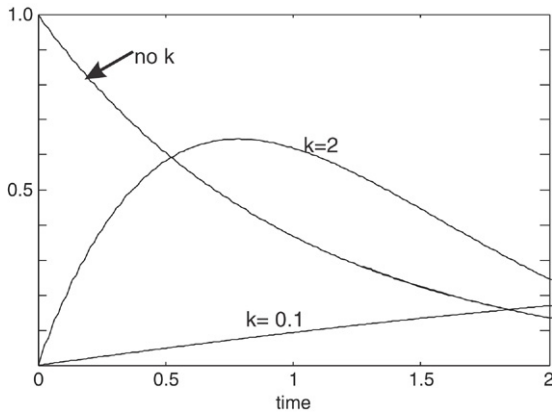


Fig. 5. The force vs time, as seen by the source for various values of k . When k gets large, the plot approaches Case 1.

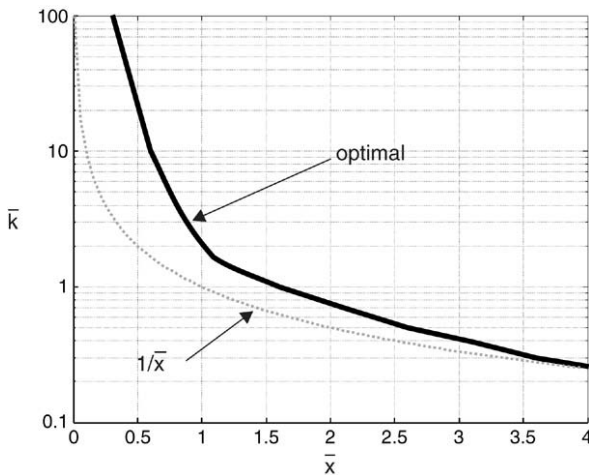


Fig. 6. This figure shows the optimal relationship (for total work output) between the dimensionless stiffness, \bar{k} , and the dimensionless stroke length, \bar{x}_{stroke} . $\frac{1}{\bar{x}_{stroke}}$ is shown for reference.

Model). The PC/104 I/O board receives input from the motor encoder and an analog signal conditioning board that buffers the signal from the analog linear potentiometer. The system runs at a frequency of 3000 Hz. Data is decimated and recorded at a rate of 300 Hz.

In the experiment, two distinct series springs were selected between $1 < \bar{k} < 2$, namely $\bar{k} = 1.1$ and $\bar{k} = 1.4$. For each \bar{k} value, several trials were run. Here, a trial consisted of giving a maximal step input to the motor amplifier and recording the sensor data as the actuator performed work throughout one maximal stroke. Data were also taken with no series elasticity.

The data from each trial were transferred over Ethernet from the PC/104 board to a desktop computer, where it was further processed in MATLAB. Position data were low-pass filtered at 100 Hz. The force applied to the output mass was calculated in two ways. First, using the spring deflection, the force was calculated as kx_{spring} . In addition, in order to check the accuracy of published spring ratings, the force was also calculated by the taking the second derivative of the mass position.

The results of the experiments are shown in Fig. 11. In Fig. 11, the series elasticity produced a power amplification of ≈ 1.3 times that of the direct drive case. In addition, Fig. 11 shows that the series elastic cases provided ≈ 3 times the work output compared to the direct drive case.

5. Discussion and future work

In both numerical simulation and experiments, we show that, for a particular level of series elasticity, amplification of work and power can be achieved for the action of accelerating a mass over a fixed stroke length. Using a simplified model, we show that an appropriate spring constant increases the energy that an actuator can deliver to a mass by a factor of 4. The series elasticity changes the actuator operating point along its force–velocity curve and therefore affects the actuator work output over a fixed stroke length. In addition, the model predicts that a series spring can store energy and deliver peak powers greater than the power limit of the source by a factor of 1.4.

Preliminary experiments are performed to test model predictions. We find qualitative agreement between the model and experimental data. The series elastic trials provided ≈ 3 times the work output compared to the direct drive case. The series elasticity trials also produced a power amplification of ≈ 1.3 times that of the direct drive case.

The model and experimental results highlight the importance of series elasticity for actuator work and power amplification across a fixed stroke length.

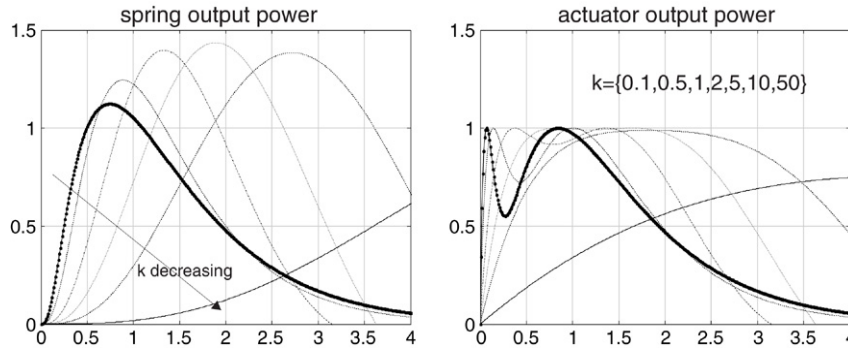


Fig. 7. Power output from the source and from the spring to the mass. Both powers are plotted as a function of time and normalized by the peak actuator power. The thick line corresponds to $k = 0.1$.

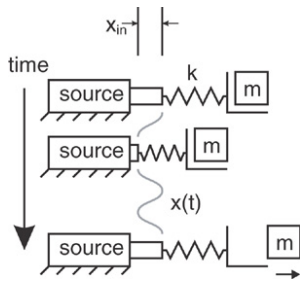


Fig. 8. A time sequence indicating how series elasticity can be used as a catchless catapult to increase energy delivery to a mass. This figure is diagrammatic only and the actual $x(t)$ would differ depending on parameters.

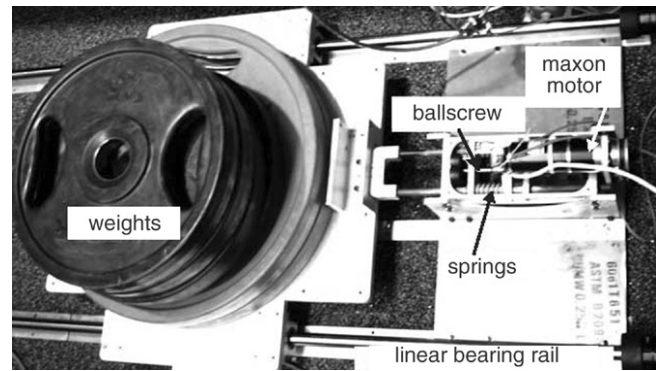


Fig. 10. A photograph of the experimental apparatus.

5.1. Work output and actuator force–velocity characteristics

Fig. 12 is a diagram illustrating how the actuator force as a function of time differs for the direct drive and series elastic cases. It is critical to note that series elasticity changes the operating velocity of the actuator. Consider the force–velocity limited actuator as shown in Figs. 1 and 3. Intuition might lead one to believe that the maximum work output can be achieved by operating at P_{max} over the entire actuator stroke (given some idealized matched load). At $P_{max} = F_{max} V_{max}/4$, the speed is $V_{opt} = V_{max}/2$, and the work done, E , over the stroke, x_{in} , is then:

$$E = P * t = P_{max} x_{in} / V_{opt} = F_{max} x_{in} / 2 = f * d. \quad (8)$$

Fig. 5 is the actual force versus displacement for the source. The area under these curves is the total work delivered to the

spring–mass load (see Fig. 4). Thus, work amplification occurs when the series elasticity allows the source to operate near P_{max} for a larger portion of the stroke.

5.2. Future work

There are many ways in which the simple model presented here can be improved. In order to better relate to biological or specific mechanical systems, additional issues need to be modeled, including actuator output mass, nonlinear (hardening) series elasticity, nonlinear force–velocity limitations, force–displacement limitations and actuator efficiency.

The results of this study highlight the need for better actuator metrics. Currently, actuators are often evaluated by their power density. Although the addition of a spring can increase peak

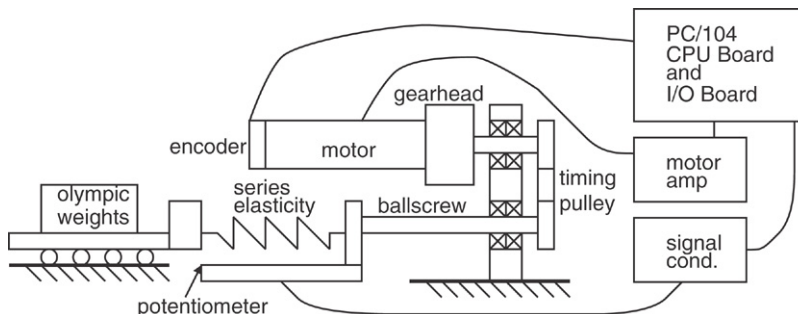


Fig. 9. A schematic of the experimental setup.

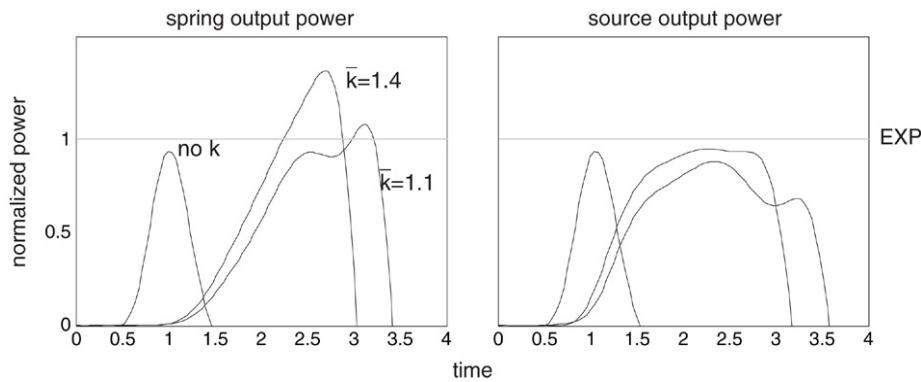


Fig. 11. Power output from the source and from the spring to the mass. Both powers are plotted as a function of time and normalized by the peak motor power. See also Fig. 7 for comparison with model results.

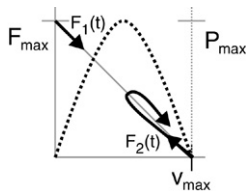


Fig. 12. This is a cartoon figure indicating how the two cases load the actuator in different ways. Of course, as k varies, the profile for Case 2 will change. For large k , the two should be essentially identical. $F_1(t)$ and $F_2(t)$ here are cartoon representations of the actual force profile, as seen in Fig. 5. The dotted curve indicates the actuator power output. For a fixed amount of time, we would like to operate near $V_{\max}/2$ for as long as possible.

power or work output for short amounts of time, the steady-state power density will always be limited by the original value of the source. We believe that there are new actuator metrics to be defined which will better represent the power and work amplification capabilities offered by series elasticity.

6. Conclusion

In both simulation and experiment, we show that series elasticity can amplify actuator work and power output over a limited stroke length. Series elasticity is an integral part of robot morphology which directly affects the system energetics and control. The effect is of critical importance to jumping and throwing robots, where minimizing limb mass while maximizing work and power output is desirable. We believe that artificial joint designs and control systems that exploit this effect will lead to artificial systems that can more closely approximate the performance of biological systems.

References

- [1] K. Kubo, Y. Kawakami, T. Fukunaga, Influence of elastic properties of tendon structures on jump performance in humans, *Journal of Applied Physiology* 87 (6) (1999) 2090–2096. Available <http://jap.physiology.org/cgi/content/abstract/87/6/2090>.
- [2] G. Ettema, Mechanical efficiency and efficiency of storage and release of series elastic energy in skeletal muscle during stretch-shorten cycles, *Journal of Experimental Biology* 199 (9) (1996) 1983–1997. Available <http://jeb.biologists.org/cgi/content/abstract/199/9/1983>.
- [3] A. Wilson, J. Watson, G. Lichtwark, A catapult action for rapid limb protraction, *Nature* 421 (2003) 35–36.
- [4] T.J. Roberts, The integrated function of muscle and tendons during locomotion, *Comparative Biology and Physiology* 133 (4) (2002) 1087–1099.
- [5] T.J. Roberts, R.L. Marsh, Probing the limits to muscle-powered accelerations: lessons from jumping bullfrogs, *Journal of Experimental Biology* 206 (15) (2003) 2567–2580. Available <http://jeb.biologists.org/cgi/content/abstract/206/15/2567>.
- [6] T.J. Roberts, R.L. Marsh, P.G. Weyand, C.R. Taylor, Muscular force in running turkeys: The economy of minimizing work, *Science* 275 (5303) (1997) 1113–1115. Available <http://www.sciencemag.org/cgi/content/abstract/275/5303/1113>.
- [7] A. Hof, B. Geelen, J. Van Den Berg, Calf muscle moment, work and efficiency in level walking: role of series elasticity, *Journal of Biomechanics* 16 (1983) 523–535.
- [8] R.M. Alexander, *Elastic Mechanisms in Animal Movement*, Cambridge University Press, 1988.
- [9] J.E. Pratt, Virtual model control of a biped walking robot, Master's Thesis, Massachusetts Institute of Technology, August 1995.
- [10] G. Pratt, M. Williamson, P. Dillworth, J. Pratt, K. Ulland, A. Wright, Stiffness isn't everything, in: *Proceedings of the Fourth International Symposium on Experimental Robotics, ISER'95*, 30 June–2 July 1995, Stanford, California.
- [11] R. Howard, Joint and actuator design for enhanced stability in robotic force control, Ph.D. Dissertation, MIT, 1990.
- [12] N. Hogan, S. Buerger, in: T. Kurfess (Ed.), *Robotics and Automation Handbook*, in: *Impedance and Interaction Control*, Ser., vol. 1, CRC Press, New York, 2005.
- [13] D. Robinson, Design and analysis of series elasticity in closed loop actuator force control, Ph.D. Dissertation, MIT, Department of Mechanical Engineering, 2000.
- [14] J.E. Pratt, Biped robot walking control, Ph.D. Dissertation, MIT, 2000.
- [15] M. Zinn, B. Roth, O. Khatib, J. Salisbury, A new actuation approach for human friendly robot design, *International Journal of Robotics Research* 23 (2004) 379–398.
- [16] M.H. Raibert, *Legged Robots That Balance*, MIT Press, Cambridge, MA, 1986.
- [17] M. Buehler, D.E. Koditschek, Analysis of a simplified hopping robot, in: *Proceedings of the IEEE International Conference on Robotics and Automation, ICRA*, 1988, pp. 817–819. Available: [Buehler88.pdf](#).
- [18] H.B. Brown, G. Zeglin, The bow leg hopping robot, in: *IEEE International Conference on Robotics and Automation*, 1998.
- [19] D.W. Robinson, J.E. Pratt, D.J. Paluska, G.A. Pratt, Series elastic actuator development for a biomimetic robot, in: *IEEE/ASME International Conference on Advanced Intelligent Mechatronics*, 1999.



Dan Paluska is a mechanical engineering Ph.D. student at the Massachusetts Institute of Technology. He works in the Biomechatronics Group at the MIT Media Laboratory. His research is focused on the advancement of actuator technologies that provide the many benefits of biological actuation. He received his BS and MS degrees from the Mechanical Engineering Department at MIT. Before joining the Biomechatronics Group, he worked in the Leg Laboratory at MIT, designing bipedal robots and series elastic actuators.



Hugh Herr is Associate Professor of Media Arts and Sciences and Health Sciences and Technology at MIT. His primary research objective is to apply the principles of muscle mechanics, neural control and human biomechanics to guide the designs of human rehabilitation and augmentation technologies. He received his BA in physics from Millersville University of Pennsylvania, and his MS in mechanical engineering from MIT, and a Ph.D. in biophysics from Harvard University.